Applied Surface Science 51 (1991) 27–33
North-Holland

ESCA characterization of copper/alumina catalysts prepared by deposition – precipitation using urea hydrolysis *

V.K. Kaushik

Research Centre, Indian Petrochemicals Corporation Limited, Vadodara-391 346, India

Ch. Sivaraj and P. Kanta Rao

Catalysis Section, Indian Institute of Chemical Technology, Hyderabad-500 007, India

Received 4 October 1990; accepted for publication 2 March 1991

X-ray photoelectron spectroscopy (XPS) has been used for the characterization of Cu/Al_2O_3 catalysts used for the dehydrogenation of ethanol and also for carbon monoxide adsorption studies. Various oxidation states of copper in oxidic and hydrogen-reduced catalysts have been identified using $Cu(2p_{3/2})$ photoelectron and Cu(LMM) Auger transitions. The $Cu(2p_{3/2})/Al(2p)$ intensity ratio from XPS data can be correlated with the copper surface area, CO adsorption capacity and reaction rate of the catalyst.

1. Introduction

Copper is one of the most interesting elements of the Periodic Table and is used as a catalyst in supported and unsupported form [1–8]. Supported copper catalysts are widely used in the dehydrogenation of lower alcohols to aldehydes and ketones, in the hydrogenolysis of aliphatic esters to the corresponding alcohols and in the oxidation of glycol to glyoxal and carbon monoxide to carbon dioxide. Copper is also one of the principal components in the low-pressure methanol synthesis catalyst. Several authors [9–17] have used spectroscopic and temperature-programmed reduction (TPR) techniques to find the nature of the species formed on the surface of these copper catalysts. Although the surface and catalytic properties of these catalysts depend on their preparation method [18,19], it is generally believed that at least two different phases of copper exist in supported oxidic catalysts–metal oxide particles and a surface phase composed of metal ions diffused into the support lattice structure.

Recently, Sivaraj and Kanta Rao [20] have shown that Cu/Al_2O_3 catalysts prepared by precipitation from a homogeneous solution (PFHS) using hydrolysis of urea possess improved catalytic properties for the dehydrogenation of ethanol to acetaldehyde. In the present investigation, electron spectroscopy for chemical analysis (ESCA) has been used to investigate the nature of the oxidation state of copper species on the surface of Cu/Al_2O_3 catalyst (with copper loadings from 9 to 34 wt%) prepared by the PFHS method. The catalytic activity of these catalysts has been correlated with surface copper species for the ethanol dehydrogenation reaction. A similar ESCA and other spectroscopic characterizations of Cu/Al_2O_3 catalyst prepared by the impregnation technique have been made by Strohmeier et al. [21].

* IPCL communication No. 168.

0169-4332/91/$03.50 © 1991 – Elsevier Science Publishers B.V. (North-Holland)

2. Experimental

2.1. Preparation of catalysts

An aqueous solution containing copper(II) nitrate of the required concentration and urea (1.2 M) was placed in a 3 ℓ round bottom glass reactor, 20 g of γ-alumina powder (200 mesh) was then added and heated to 90–95 °C with constant stirring. The pH of the solution was measured at different intervals of time using a digital pH meter. After the precipitation was complete (pH = 7.5), the solution was filtered in a Buchner funnel, the precipitate washed several times with distilled water and dried at 110 °C for 24 h. The catalyst precursors contained besides γ-Al_2O_3, $Cu_2(OH)_3NO_3$ or $Cu_2(OH)_3NO_3$ and $Cu(OH)_2$ depending upon the copper content. The supported oxide catalysts were then obtained by calcining the catalyst precursors at 400 °C for 24 h. The copper content of the calcined Cu/Al_2O_3 catalysts varied between 9 and 34 wt%. A detailed discussion on the precipitation from homogeneous solution and the precursors formed at different copper loadings and the phase composition of the calcined catalysts is presented elsewhere [20].

2.2. Activity measurements

A differential flow microreactor, operating under normal atmospheric pressure and interfaced to a gas chromatograph by a six-way sampling valve was used to measure the activity of the catalysts. About 0.1 g of the catalyst was secured between two glass wool plugs inside a borosilicate glass reactor of 10 mm ID fitted with a thermowell and an electrically heated vertical tubular furnace. The average particle size (0.5 mm) was chosen so as to eliminate mass-transfer effects. High-purity nitrogen (99.9%) further dried with a molecular sieve (4A) was passed through two saturators containing pure ethanol maintained at the appropriate temperature to achieve the desired partial pressure. All the conversion rates were measured under steady-state conditions with the help of the equation $X = r(W/F)$, where r is the rate in mol h^{-1} g^{-1} catalyst, W is the weight of the catalyst in g, and F is the flow-rate of the reactant in mol h^{-1}. The extent of conversion X was maintained below 20% and a straight line was obtained by plotting X against W/F for each catalyst. The rates were calculated from the slopes of these lines.

2.3. Carbon monoxide chemisorption and Cu metal area

A conventional high-vacuum system with a facility for reducing the sample in-situ by flowing hydrogen was used for the CO chemisorption/N_2O decomposition study. The standard pretreatment procedure employed was the reduction of the catalyst sample (about 0.5 g) for 5 h at 250 °C, followed by evacuation for 2 h (10^{-6} Torr) at the same temperature prior to CO chemisorption/N_2O decomposition. The catalyst chamber was then cooled to ambient temperature (25 °C) and the evacuation was continued for a further 1 h at the temperature of CO chemisorption (25 °C). Introducing purified CO (Matheson 99.9%), CO adsorption isotherms were generated representing total CO uptakes. Adsorptive decomposition of N_2O was carried out at 90 °C for 5 h. Details of the experimental procedure are described elsewhere [20,22].

2.4. XPS measurements

A Vacuum Generators ESCALAB MK II spectrometer with a Mg Kα (1253.6 eV) radiation source was used for the measurement of copper XPS. The anode was operated at 10 kV and 10 mA and the vacuum in the analysis chamber was ensured to be better than 5×10^{-8} mbar. Catalyst samples were dusted on double-sided adhesive tape and mounted on the sample holder. These samples were transferred to the fast-entry lock of the spectrometer. Each catalyst sample was kept overnight in the preparation chamber before being transferred to the analysis chamber for X-ray photoelectron spectroscopic (XPS) analysis. The Al(2p) photoelectron line at 74.5 eV from the catalyst support was taken as reference for correction of the charging effect. This binding energy reference gave C(1s) at 285.0 ± 0.1 eV from pump oil contamination. The data were collected and analysed on an Apple IIe microcomputer interfaced to the

Table 1
XPS and Auger line positions for copper standards

Element/ compound	$Cu(2p_{3/2})$ [a] BE (eV)	Satellite to main line intensity	Cu(LMM) KE (eV)	Auger parameter (ref. [23])	Auger parameter (ref. [21])
Cu	932.7 (1.5)	–	918.5	1851.2	1851.1
Cu_2O	932.8 (1.7)	–	916.5	1849.3	1849.1
CuO	933.8 (3.5)	0.41	917.6	1851.4	1851.6
$CuAl_2O_4$	935.0 (3.1)	1.10	916.5	–	1851.5

[a] Values in parentheses are FWHM.

spectrometer. ESCA binding energies and intensity ratios are the average of three different runs. It is to be noted that the 3p lines of copper overlap [#1] with the Al(2p) line and hence intensity from Cu(3p) photoelectron lines was unavoidable in the measurement of the integrated intensity of the Al(2p) line used in the $Cu(2p_{3/2})/Al(2p)$ intensity ratio. Before peak areas of these photoelectron lines were estimated, linear background subtraction was performed.

3. Results and discussions

Kaushik in his previous study [23] has made $Cu(2p_{3/2})$ photoelectron and Cu(LMM) Auger line measurements for Cu, Cu_2O and CuO standards of copper. The line positions and chemical-state parameters for these compounds are close (within estimated uncertainty) to the values reported by Strohmeier et al. [21]. However, $CuAl_2O_4$ is also a useful reference compound to model the extreme situation which exist on Cu/Al_2O_3 catalysts. Strohmeier et al. [21] reported the $Cu(2p_{3/2})$ line at 935.0 eV and a satellite-to-main line intensity ratio of 1.10 for this compound. The values shown in table 1 have been used in assigning the chemical state in the present study.

Thus, based on the studies of Kaushik [23] and Strohmeier et al. [21] it can be concluded that Cu° and Cu^+ cannot be distinguished by XPS measurements and Cu^{2+} from CuO and $CuAl_2O_4$ cannot be distinguished from their Auger parameter values. However, the Auger lines of Cu° and Cu^+ are separated by approximately 2 eV and the photoelectron and Auger lines of CuO and $CuAl_2O_4$ are separated by approximately 1 eV each making a clear distinction between Cu°/Cu^+ and Cu^{2+} from $CuO/CuAl_2O_4$. Also the satellite intensity of $CuAl_2O_4$ is much stronger compared to that of CuO and Cu^{2+} can be easily distinguished from Cu° or Cu^+ by their line shape, photoelectron and Auger line positions.

The Cu(2p) photoelectron spectra of the catalysts studied are shown in fig. 1 and their photoelectron line positions are given in table 2. It can be seen from the binding energy values of all the calcined catalysts (obtained after calcination of catalyst precursors at 400 °C for 24 h) that these values vary with the catalyst sample (copper loading) and lie between CuO and $CuAl_2O_4$ upto 16 wt% copper loading on catalysts. At higher copper loading photoelectron lines due to CuO and Cu_2O were observed on the catalyst surface with only CuO surface species detected on the catalyst with 21.6 wt% copper. As $CuAl_2O_4$ shows more intense satellite structure, satellite intensities were measured to indicate which species are quantitatively more present on catalysts with copper loading upto 16 wt%. Such satellite-to-main line intensity values given in table 2 show that initially the $CuAl_2O_4$ phase was more present on the catalyst surface (8.9 wt%) and gradually CuO is built up on the catalyst surface such that at 21.6 wt% copper loading only CuO species were detected and no $CuAl_2O_4$ phase was seen on the catalyst surface. This shows that at lower copper loading copper metal interacts with the support to form a spinel $CuAl_2O_4$ structure on the catalyst surface.

[#1] Because of this overlap, measured Al(2p) areas are overestimated. Thus, the estimated intensity ratio will be lower than the realistic value but it will not affect the trend of copper dispersion.

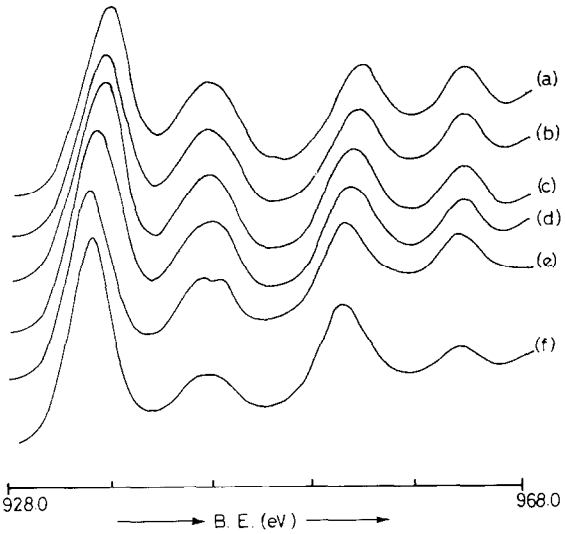

Fig. 1. Cu(2p) photoelectron spectra of catalysts with (a) 8.9, (b) 13.1, (c) 16.0, (d) 21.6, (e) 27.1 and (f) 34.2 wt% copper.

As loading is increased, the spinel $CuAl_2O_4$ phase disappears from the surface and CuO phase builds up on the surface. However, at much higher loading Cu_2O phase has also been seen on the catalyst along with the CuO phase. As CuO reduces readily to Cu_2O [24,25], the possibility of CuO reduction to Cu_2O cannot be completely ruled out during XPS analysis.

The [Cu($2p_{3/2}$) + satellite]/Al(2p) ESCA intensity ratios which reflect the copper dispersion on alumina support are also given in the last column on table 2 for oxidic catalysts. These values indicate that initially this intensity ratio increases with the increase in copper loading with maxima at 21.6 wt% and then declines with the increase in copper loading probably because of the formation of large CuO crystallites. Detection of bulk CuO in catalysts with 21.6 wt% copper loadings were confirmed by the XRD patterns of these catalysts.

3.1. Ethanol dehydrogenation and carbon monoxide adsorption study

Reaction of ethanol on Cu/Al_2O_3 catalysts gave acetaldehyde and ethyl acetate (dehydrogenation products) and ethene and diethyl ether (dehydration products). The γ-Al_2O_3 used as support exhibited only dehydration activity at 250 °C [26]. When copper was added, dehydrogenation activity was evident, the activity depending upon the copper content. The selectivity for acetaldehyde plus ethyl acetate increased from 94% at a copper loading of 8.9 wt% to 98%–100% with further increase in copper loading to 34.2 wt%. The catalyst with 8.9 wt% copper has a selectivity of only 6% to ethene plus diethyl ether. While the selectivities to the dehydrogenation products increased with increase in copper loading, those for the dehydration products decreased correspondingly. Ethyl acetate selectivities varied from 0.2% to 7% depending on the copper content in the catalyst.

The results of the ethanol dehydrogenation reaction on Cu/Al_2O_3 catalysts expressed in terms of the initial rate (per gram catalyst) are shown in fig. 2a as a function of copper loading. It can be seen from fig. 2 that the dehydrogenation activity for ethanol increases with the copper loading upto 21.6 wt% and then decreases with a further in-

Table 2
ESCA results on Cu/Al_2O_3 catalysts

Copper catalyst (copper wt%)	Cu($2p_{3/2}$) [a] BE (eV)	Satellite [b] to main line intensity	Surface phases	ESCA intensity ratio Cu($2p_{3/2}$)/Al(2p)
8.9	934.8	0.58	CuO, $CuAl_2O_4$	3.50
13.1	934.6	0.51	CuO, $CuAl_2O_4$	4.04
16.0	934.5	0.49	CuO, $CuAl_2O_4$	4.20
21.6	934.0	0.41	CuO	4.35
27.1	933.7	0.35	CuO, Cu_2O	3.90
34.2	933.8	0.27	CuO, Cu_2O	3.25

[a] BE were reproducible to ±0.3 eV for catalysts upto 21.6 wt% copper and ±0.2 eV for other catalysts.
[b] Satellite intensities were reproducible within ±0.04 of the main line intensity.

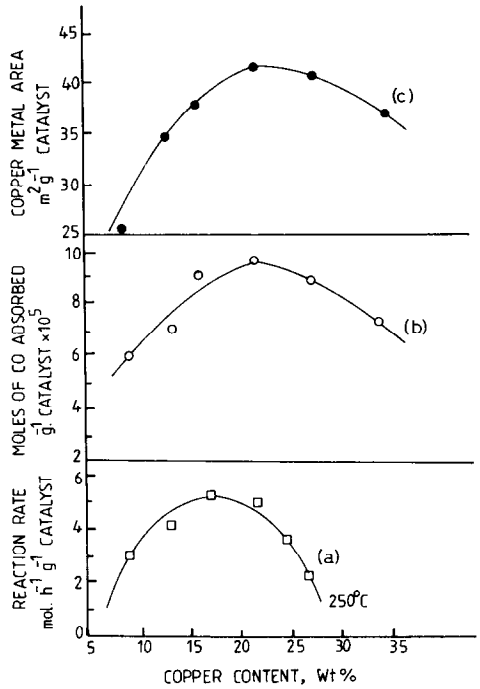

Fig. 2. (a) Dehydrogenation rate of ethanol, (b) total carbon monoxide adsorption and (c) copper area as a function of copper loading in Cu/Al_2O_3 catalysts.

crease in copper loading. Similarly, the total carbon monoxide adsorption also increases upto a copper loading of 21.6 wt% and then decreases with the increase in copper loading (fig. 2b). This optimum composition corresponds to the maximum number of active species as well as to the maximum copper surface area.

From nitrous oxide decomposition data, the copper metal areas were calculated and the results are shown in fig. 2c as a function of copper loading. The copper metal area expressed in m^2 g^{-1} catalyst increases with the copper loading upto 21.6 wt% and then decreases with the increase in copper loading indicating that at this loading the "maximum number of copper species are available on the catalyst surface and the formation of a monolayer [#2] of copper species on alumina support can be expected". An important observation from the copper area data is that even at full monolayer coverage only 29.4% of the total copper atoms are available on the catalyst surface at 21.6 wt% Cu. The decrease in copper area with further increase in copper content in the catalyst may be due to build-up of large copper crystallites as well as pore mouth blocking. XPS data for catalyst with 21.6 wt% copper from table 2 shows that at this loading all copper species on the catalyst surface are CuO and the [$Cu(2p_{3/2})$ + satellite]/Al(2p) intensity ratio is maximum for this catalyst. This also indicates that the maximum number of copper species are available on the surface of this catalyst.

[#2]Here the term "monolayer" has not been applied to indicate complete coverage of the active support surface; rather it indicates covering of certain patches of the active support surface.

3.2. Reduction studies

Reduction characteristics of supported metal oxides are quite different from the bulk oxides because of metal–support interaction and change in dispersion. It was therefore interesting to investigate the reducibility of Cu/Al_2O_3 catalysts. In the present investigation, the catalysts reported in table 3 were reduced at 250 °C for 5 h in hydrogen atmosphere. Unlike the Cu(2p) photoelectron spectra of oxidic catalysts, the XPS of these catalysts do not show satellite structure indicating that Cu^{2+} species are not present on the surface of reduced catalysts. Hence, reduction treatment of Cu/Al_2O_3 catalyst reduces Cu^{2+} to Cu° and Cu^{+} species. The XPS and Auger measurements given in table 3 show that for copper loading upto 21.6 wt% reduction takes place to Cu° and Cu^{+}, while above this loading, it com-

Table 3
ESCA data on reduced catalysts

Copper catalyst (copper wt%)	Cu ($2p_{3/2}$) BE (eV)	Cu (LMM) KE (eV)	Surface phase	$Cu(2p_{3/2})/Al(2p)$ intensity ratio	
				Reduced	Oxidic
16.0	932.8 ± 0.2	916.4 ± 0.2 918.5 ± 0.2	Cu, Cu_2O	1.93	4.20
21.6	932.7 ± 0.2	916.3 ± 0.3 918.4 ± 0.2	Cu, Cu_2O	1.95	4.35
27.1	932.7 ± 0.2	918.5 ± 0.2	Cu	1.77	3.90

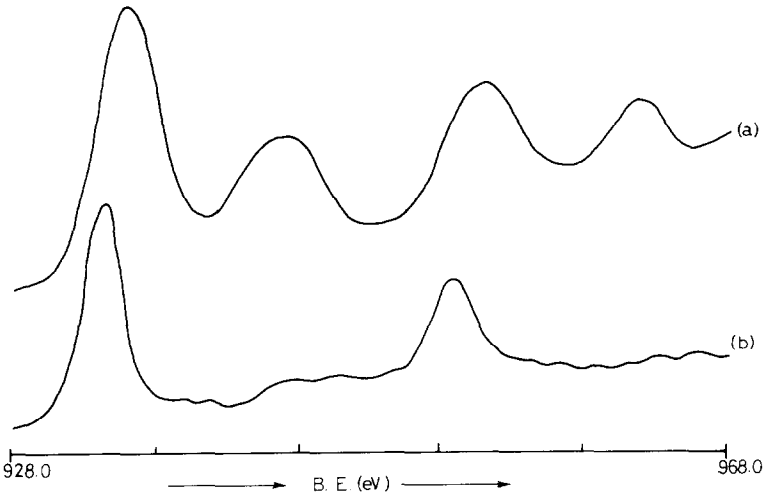

Fig. 3. Cu(2p) photoelectron spectra of (a) oxidic and (b) reduced catalysts with copper loading 21.6 wt%.

pletely reduces to Cu°. The $Cu(2p_{3/2})/Al(2p)$ ESCA intensity ratios for these hydrogen-reduced catalysts have been compared with corresponding values for oxidic catalysts in table 3. This comparison shows that the ratio decreases approximately 45% compared to the corresponding oxidic catalyst value, indicating a decrease in copper dispersion on reduction. Figs. 3 and 4 show XPS in Cu(2p) and Al(2p) regions for oxidic and hydrogen-reduced catalysts with 21.6% copper content. As the Al(2p) photoelectron line includes overlap due to Cu(3p) lines, fig. 4 shows how copper dispersion on the catalyst surface reduces on hydrogen-reduced catalysts. This reduction in dispersion may be attributed either to diffusion of copper into the substrate or to the formation of large copper metal particles.

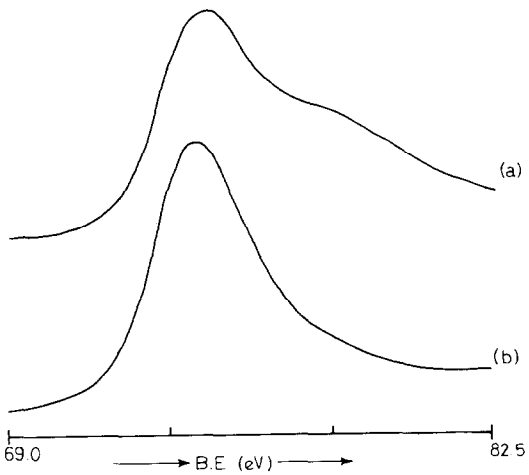

Fig. 4. Al(2p) photoelectron spectra of (a) oxidic and (b) reduced catalysts with copper loading 21.6 wt%.

4. Conclusions

Based on the present study, the following conclusions can be drawn for PFHS prepared Cu/Al_2O_3 catalysts:

(1) At low metal loading and at a calcination temperature of 400°C, formation of a "surface spinel" $CuAl_2O_4$ phase predominates while at higher metal loading, segregation of bulk-like CuO occurs.

(2) XPS data shows that a catalyst with only CuO species on its surface and having the highest Cu $(2p_{3/2})/Al(2p)$ intensity ratio shows maximum dehydrogenation activity as well as maximum CO adsorption, i.e. a catalyst with a highly dispersed CuO surface phase is most suitable for the dehydrogenation reaction of ethanol.

(3) The hydrogen-treated (250°C, 5 h) Cu/Al_2O_3 catalysts show progressive reduction of Cu^{2+} to lower oxidation state together with a concomitant decrease of the Cu/Al atomic ratio at the sample

surface (comparison given in the last two columns of table 3). This may be attributed to the diffusion of copper into the substrate or the formation of metal crystallites bigger than the escape depth of the emitted electrons. Similar decreases in the intensity ratio have been reported by Stohmeier et al. [21].

Acknowledgements

The authors thank Dr. T.S.R. Prasada Rao for helpful discussions and valuable advise in the preparation of the manuscript. The encouragement and support provided by Dr. I.S. Bhardwaj, Director (R&D), Indian Petrochemicals Corporation Limited, Vadodara and Dr. A.V. Rama Rao, Director, Indian Institute of Chemical Technology, Hyderabad is gratefully acknowledged. We are also grateful to the management of Indian Petrochemicals Corporation Limited for permitting us to publish this work.

References

[1] R. Pearce and W.R. Petterson, Catalysis and Chemical Processes (Hill, Glassgow, 1981) p. 279.
[2] Ch. Sivaraj, B. Mahipal Reddy and P. Kanta Rao, Appl. Catal. 45 (1988) L11.
[3] J.W. Evans, M.S. Wainwright, N.W. Cant and D.L. Trimm, J. Catal. 88 (1984) 203.
[4] J.W. Evans, P.S. Casey, M.S. Wainwright, D.L. Trimm and N.W. Cant, Appl. Catal. 7 (1983) 31.
[5] C.L. Thomas, Catalysis Process and Proven Catalysts (Academic Press, New York, 1970) p. 198.
[6] F. Severino, J. Brinto, O. Carias and J. Laine, J. Catal. 102 (1986) 172.
[7] G.C. Chinchen, P.J. Denny, J.R. Hennings, M.S. Spencer and K.C. Waugh, Appl. Catal. 36 (1988) 1, and references therein.
[8] V.K. Kaushik and M. Ravindranathan, Appl. Catal. 47 (1989) 343.
[9] G.N. Asimov and O.V. Krylov, Kinet. Katal. 12 (1971) 403.
[10] K.S. Chung and F.M. Massoth, J. Catal. 64 (1980) 320.
[11] R.L. Chin and D.M. Hercules, J. Phys. Chem. 86 (1982) 360.
[12] M. Wu and D.M. Hercules, J. Phys. Chem. 83 (1979) 2003.
[13] R.M. Friedman, J.J. Freeman and F.W. Lytle, J. Catal. 55 (1978) 10.
[14] J. Cunningham, D. McNamara, J.L.G. Fierro and S. O'Brien, Appl. Catal. 35 (1987) 381.
[15] W.A.M. Robinson and J.C. Mol, Appl. Catal. 44 (1988) 165.
[16] R. Vetrievel, K. Sheshan, K.R. Krishnamurthy and T.S.R. Prasada Rao, Bull. Mater. Sci. 9 (1987) 75.
[17] R. Vetrievel, K.V. Rao, K. Sheshan, K.R. Krishnamurthy and T.S.R. Prasada Rao, in: Proc. 9th Int. Congr. on Catalysis, Calgary, 1988, p. 1766.
[18] M.A. Kohler, J.C. Lee, D.L. Trimm, N.W. Cant and M.S. Wainwright, Appl. Catal. 31 (1987) 309.
[19] Ch. Sivaraj, B. Rama Rao, M. Raza Hussain and P. Kanto Rao, in: Proc. 2nd Indo-Soviet Seminar on Recent Advances in Catalysis and Catalytic Reaction Engineering, RRLAB, Hyderabad, India, November 1986, Ed. P. Kanta Rao, p. 492.
[20] Ch. Sivaraj and P. Kanta Rao, Appl. Catal. 45 (1988) 103.
[21] B.R. Strohmeier, D.E. Leyden, R.S. Field and D.M. Hercules, J. Catal. 94 (1985) 514.
[22] J.J.F. Scholten, An. Quim. 81 (1985) 485.
[23] V.K. Kaushik, Spectrochim. Acta 44B (1989) 581.
[24] B. Wallbank, C.E. Johnson and I.G. Main, J. Electron Spectrosc. Rel. Phen. 4 (1974) 263.
[25] A. Rosencwaig and G.K. Wertheim, J. Electron Spectrosc. Rel. Phen. 1 (1972) 493.
[26] Ch. Sivaraj, B. Prabhakar Reddy, B. Rama Rao and P. Kanto Rao, Appl. Catal. 24 (1986) 25.